

Thermal model at RHIC, part II: elliptic flow and HBT radii ¹

Wojciech Broniowski, Anna Baran, and Wojciech Florkowski

The H. Niewodniczański Institute of Nuclear Physics, PL-31342 Cracow, Poland

Abstract. We continue the analysis of the preceding talk with a discussion of the elliptic flow and the Hanbury-Brown–Twiss pion correlation radii. It is shown that the thermal model can be extended to describe these phenomena. The description of the elliptic flow involves an appropriate deformation of the freeze-out hyper-surface and flow velocity. The obtained results agree reasonably with the data for soft (< 2 GeV) transverse momenta. For the pionic HBT correlation radii the experimental feature that $R_{\text{out}}/R_{\text{side}} \simeq 1$ is naturally obtained. The reproduction of individual R_{side} and R_{out} can be achieved with the inclusion of the excluded volume corrections, which effectively increase the radii by $\sim 30\%$.

INTRODUCTION

In the preceding talk [1], from now on referred to as (I), it has been shown that the thermal approach is successful in the description of the particle ratios and p_{\perp} -spectra at RHIC. Here we continue our investigation, studying azimuthal asymmetry of the spectra and the pionic Hanbury-Brown–Twiss correlation radii.

ELLIPTIC FLOW

When the nuclei collide at non-zero impact parameter, $b \neq 0$, the momentum distribution of the produced particles carries azimuthal asymmetry. In general, at mid-rapidity ($y = 0$) we may write the following Fourier decomposition in the azimuthal angle ϕ , measured from the reaction plane:

$$\left. \frac{dN}{d^2p_{\perp} dy} \right|_{y=0} = \left. \frac{dN}{2\pi p_{\perp} dp_{\perp} dy} \right|_{y=0} (1 + 2v_2 \cos 2\phi + 2v_4 \cos 4\phi + \dots). \quad (1)$$

The sines are absent due to the symmetry condition $\phi \rightarrow -\phi$, which is simply the reflexion with respect to the reaction plane, while the coefficients of cosines with odd multiples of ϕ vanish for the case of symmetric nuclei and at $y = 0$, when the symmetry

¹ Talk presented at II International Workshop on Hadron Physics, *Effective Theories of Low-Energy QCD*, 25-29 September 2002, University of Coimbra, Portugal

$\phi \rightarrow \pi - \phi$ holds. The elliptic-flow coefficient, v_2 , can therefore be computed as

$$v_2 = \frac{\int_0^{2\pi} \frac{dN}{d^2p_\perp dy} \Big|_{y=0} \cos 2\phi d\phi}{\int_0^{2\pi} \frac{dN}{d^2p_\perp dy} \Big|_{y=0} d\phi}. \quad (2)$$

The value of v_2 is an important signature of the physics occurring in heavy-ion collisions. Most importantly, its non-vanishing value indicates that the production mechanism is not a simple composition of nucleon-nucleon collisions, since in that case the asymmetry of production in each such collision would average out practically to zero. Thus, interactions with other particles (rescattering, asymmetric collective flow, ...) are necessary to generate non-vanishing v_2 . In hydrodynamical approaches the elliptic flow has been analyzed in many papers, see *e.g.* [2, 3, 4, 5, 6]). The coefficient v_2 depends on the impact parameter, b , on the transverse momentum p_\perp , as well as, obviously, on the type of the considered particle. All these dependences are measured at RHIC. The impact parameter, b , is traded for the experimentally more useful centrality parameter, c , which to a very good accuracy is given by [7]

$$c \simeq \frac{b^2}{(2R)^2}. \quad (3)$$

There are two basic empirical facts from RHIC which we will use in our approach. Firstly, v_2 is positive [8, 9, 10, 11, 12, 13, 14, 15, 16, 17], which means that the collective flow is faster in the reaction plane than out-of-plane. Secondly, the measurement [18] of the azimuthal dependence of the R_{side} pion HBT radius shows, that the shape of the system at freeze-out is elongated out of the reaction plane. We will now use these two facts in our choice of the parameterization of the hypersurface at freeze-out. A natural extension of Eq. (I.6) is to introduce the azimuthal shape asymmetry,

$$\begin{aligned} r_x &= \rho_{\text{max}} \sqrt{1 - \varepsilon} \cos \phi, \\ r_y &= \rho_{\text{max}} \sqrt{1 + \varepsilon} \sin \phi, \end{aligned} \quad (4)$$

with r_z and t kept as in the symmetric case of Eq. (I.6) of paper (I). Our convention is that r_x lies in the reaction plane, and r_y is perpendicular to the reaction plane. For positive ε this produces elongation out of the reaction plane, as seen in the experiment. The four-velocity of Eq. (I.3) is modified as follows:

$$\begin{aligned} u_x &= \frac{1}{N} r_x \sqrt{1 + \delta} \cos \phi, \\ u_y &= \frac{1}{N} r_y \sqrt{1 - \delta} \sin \phi, \\ u_z &= \frac{1}{N} r_z, \\ u_t &= \frac{1}{N} t. \end{aligned} \quad (5)$$

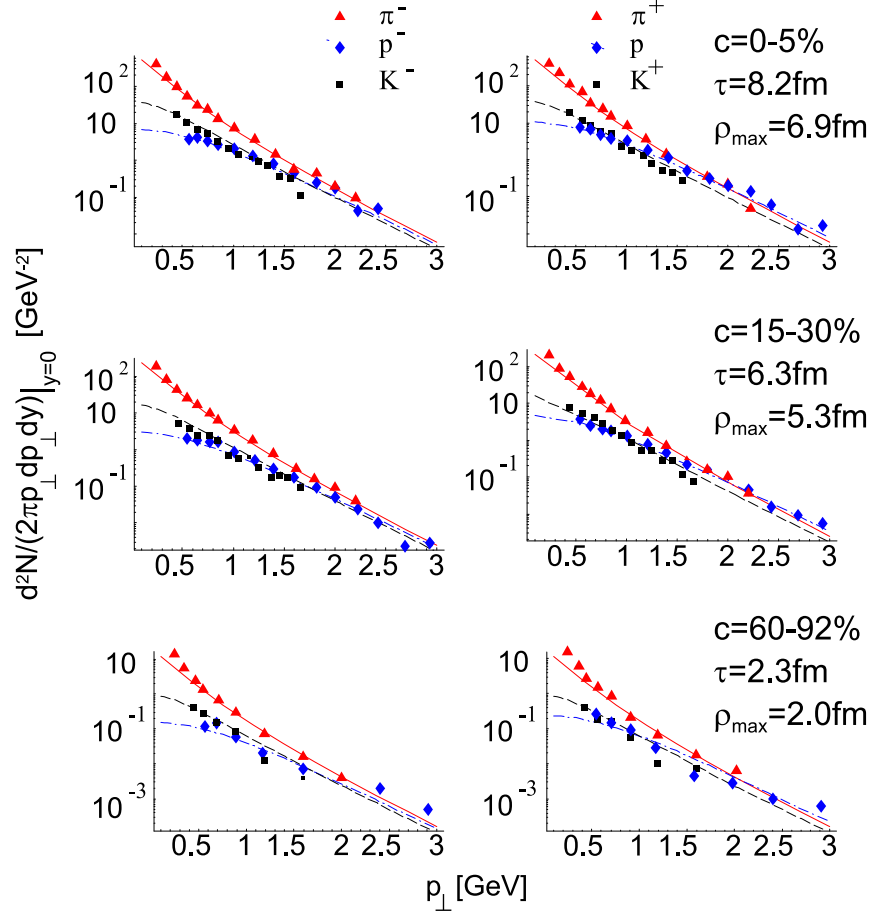


FIGURE 1. The model fit of the pion, kaon, and proton spectra to the PHENIX data for $\sqrt{s_{NN}} = 130$ GeV [15] at three centrality bins, arranged top to bottom. Negative (positive) hadron are shown in the left (right) side. The optimum values of the size parameters τ and ρ_{\max} are given for each centrality bin.

The normalization N is such that $u^\mu u_\mu = 1$. Positive δ means faster flow in the reaction plane, which corresponds to positive v_2 . Certainly, the choice (4,5) is by no means unique, but it grasps the essential empirical features.

The modified expansion model has four geometric parameters: τ , ρ_{\max} , ε and δ . These parameters depend on the centrality parameter, c . Fortunately, the effect of ε and δ on the ϕ -averaged spectra, $dN/(2\pi p_\perp dp_\perp dy)|_{y=0}$, is negligible and enters at the level of a few percent. Thus we may first fit τ and ρ_{\max} to the ϕ -averaged p_\perp -spectra at various centrality parameters, assuming for the moment vanishing ε and δ . The result is shown in Fig. 1. We note that the fit works as good as for the most-central case presented in (I). The optimum values of parameters are collected in Table 1, where they are also compared to the minimum-bias fit and the joint fit to the most central PHENIX [15] and STAR [19] data. In fact, the qualitative dependence of τ and ρ_{\max} on c is as expected: the larger c , *i.e.* the more peripheral collision, the smaller values of the size parameters. Figure 2 visualizes this dependence. In Table 1 we also list the ratio of ρ_{\max}/τ , and the maximum and average values of the flow parameter, β . Interestingly, these quantities

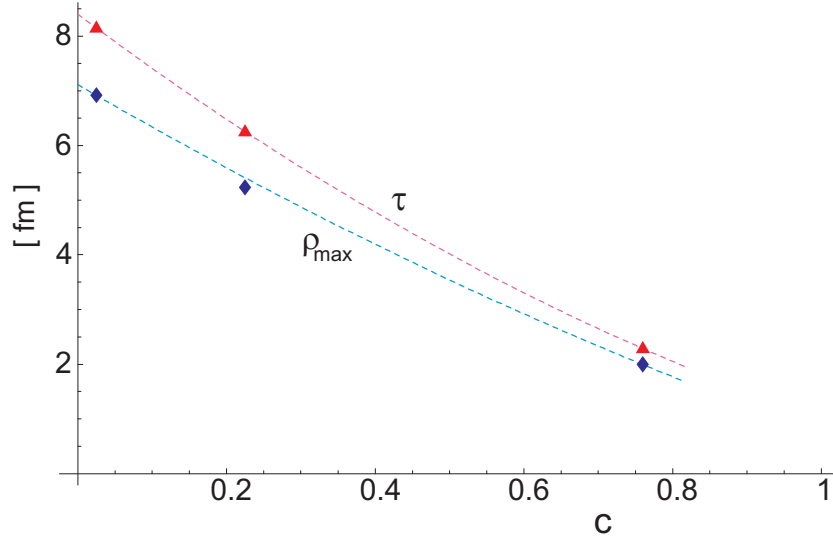


FIGURE 2. The dependence of the size parameters τ and ρ_{\max} on the centrality parameter c , as fitted to the PHENIX data on ϕ -integrated p_{\perp} -spectra at $\sqrt{s_{NN}} = 130$ GeV [15].

depend very weakly on c . They are defined as follows:

$$\beta_{\perp}^{\max} = \frac{\rho_{\max}}{\sqrt{\tau^2 + \rho_{\max}^2}},$$

$$\langle \beta_{\perp} \rangle = \int_0^{\rho_{\max}} r dr \frac{r}{\sqrt{\tau^2 + r^2}} / \int_0^{\rho_{\max}} r dr. \quad (6)$$

Ideally, the dependence of the ε parameter on c should come from the measurement of R_{side} at various centralities. Then the model evaluation of this quantity would allow to fit independently $\varepsilon(c)$ to the data. We hope to be able to proceed in such a manner in the future. Unfortunately, no necessary experimental results are available at the moment. In this circumstance we take a reasonable theoretical estimate for $\varepsilon(c)$ based on Ref. [4], which leads to $\varepsilon = 0.1, 0.21, \text{ and } 0.35$ in the centrality bins $0 - 15\%$, $15 - 30\%$,

TABLE 1. Comparison of the size parameters obtained by fitting particle spectra at various values of the centrality parameter c . Their ratio, as well as the maximum and average value of the flow parameter, β_{\perp} , are also given.

c [%]	PHENIX @130GeV				PHENIX+STAR
	min. bias	0-5	15-30	60-92	@130GeV 0-5/0-6
τ [fm]	5.6	8.2	6.3	2.3	7.7
ρ_{\max} [fm]	4.5	6.9	5.3	2.0	6.7
ρ_{\max}/τ	0.81	0.84	0.84	0.87	0.87
β_{\perp}^{\max}	0.62	0.64	0.64	0.66	0.66
$\langle \beta_{\perp} \rangle$	0.46	0.47	0.47	0.48	0.48

and 30 – 60%, respectively. Finally, the parameter δ is obtained by fitting the model predictions to the v_2 measurements. Our approach includes, as described in detail in (I), the decays of resonances. The calculation is straightforward and very similar to the one discussed in (I), although takes a much longer computer time due to a lower degree of symmetry. The technicalities will be presented elsewhere. The simplified results for v_2 presented here include all resonances up to $m_\Delta = 1.232$ GeV, and do not take into account three-body decays.

Figure 3 shows the result of our calculation for three different centrality bins. The elliptic flow coefficient grows with the momentum. It continues to grow for large momenta, where saturation is seen in the experiment, however the thermal model cannot be trusted at momenta larger than about, say, 2 GeV, where hard dynamics is important. We observe that the effects of resonance decays, large in both the numerator and denominator of Eq. (2), cancel to a large degree in the ratio, and the net effect in v_2 is small. The dependence of v_2 on centrality for various transverse-momentum bins is shown in

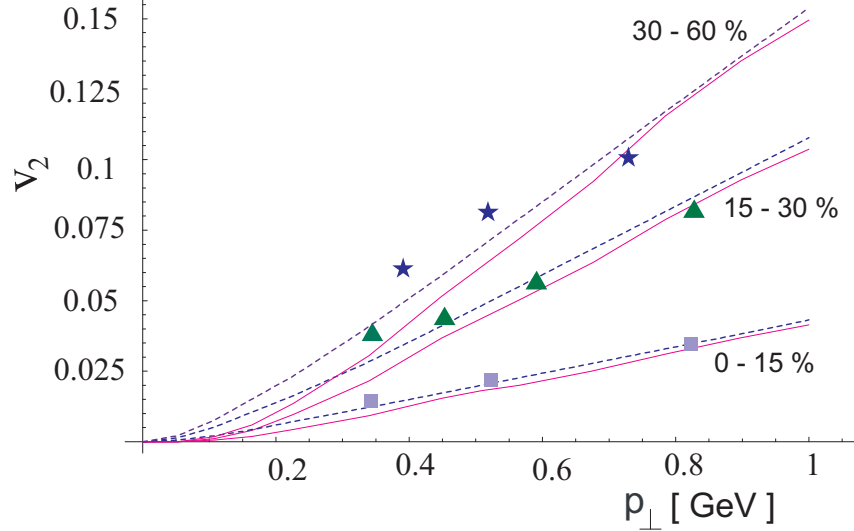


FIGURE 3. Dependence of v_2 (accumulated from all particle species) on the perpendicular momentum, p_\perp , for three centrality bins: 0 – 15% (bottom), 15 – 30% (middle), and 30 – 60% (top). Thick (thin) lines correspond to the calculation with (without) resonance decays. Experimental points come from the PHENIX collaboration at $\sqrt{s_{NN}} = 130$ GeV [17]. The taken values for the shape-asymmetry parameter ε are, from the lowest to highest centrality bin, 0.1, 0.21, and 0.35, while the fitted values of the flow-asymmetry parameter δ are 0.145, 0.34, and 0.35, respectively.

Fig. 4. We note that our calculation works well except large c and p_\perp , *i.e.* except for high-momentum particles from most peripheral collisions.

In Fig. 5 we compare the model predictions for v_2 integrated over c for identified particles: pions, kaons, and protons. The general characteristics, with lighter particles having larger v_2 , are reproduced. The agreement is not satisfactory only for the case of protons at lowest centrality, where the data is compatible with zero.

To summarize this part we note that

1. Elliptic flow can be introduced in the thermal approach by suitably modifying the freeze-out hypersurface.

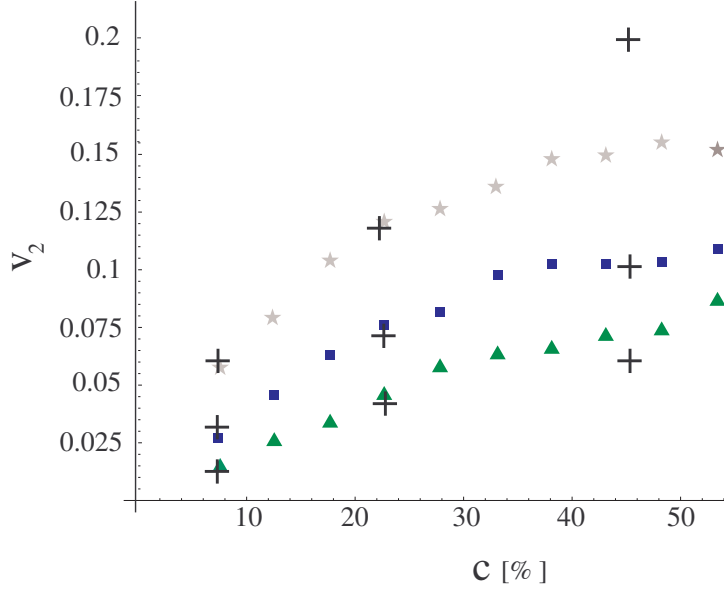


FIGURE 4. Dependence of v_2 (accumulated from all particle species) on the centrality parameter for various transverse-momentum bins: 0.4–0.6 GeV (bottom), 0.6–1 GeV (middle), and 1–2.5 GeV (top). Crosses show the model calculation, while other symbols are the experimental points from the PHENIX collaboration at $\sqrt{s_{NN}} = 130$ GeV [17]. The ε and δ parameters are the same as in Fig. 3.

2. The shape-deformation parameter, $\varepsilon(c)$, should and hopefully will be taken independently from future data on the azimuthal asymmetry of the R_{side} HBT correlation radius at various centralities.
3. The velocity-asymmetry parameter, $\delta(c)$, can be fitted to reproduce v_2 . Predictions for identified-particle v_2 follow and are reasonable.
4. The p_{\perp} -dependence shows a monotonic growth, which agrees with the data at lower values of p_{\perp} , but certainly fails to produce saturation at large momenta, where the thermal approach is not applicable.
5. Resonance decays do not have a very large effect on v_2 .

HBT RADII

Now we pass to the description of the pionic Hanbury-Brown–Twiss correlation radii (for a review of the problem see, *e.g.*, [20]). The studied object is the two-particle correlation function for identical particles, in the present case $\pi^+\pi^+$ or $\pi^-\pi^-$. It is given by

$$C(\vec{q}, \vec{P}) = \frac{\{n_{\vec{p}_1} n_{\vec{p}_2}\}}{\{n_{\vec{p}_1}\} \{n_{\vec{p}_2}\}}, \quad (7)$$

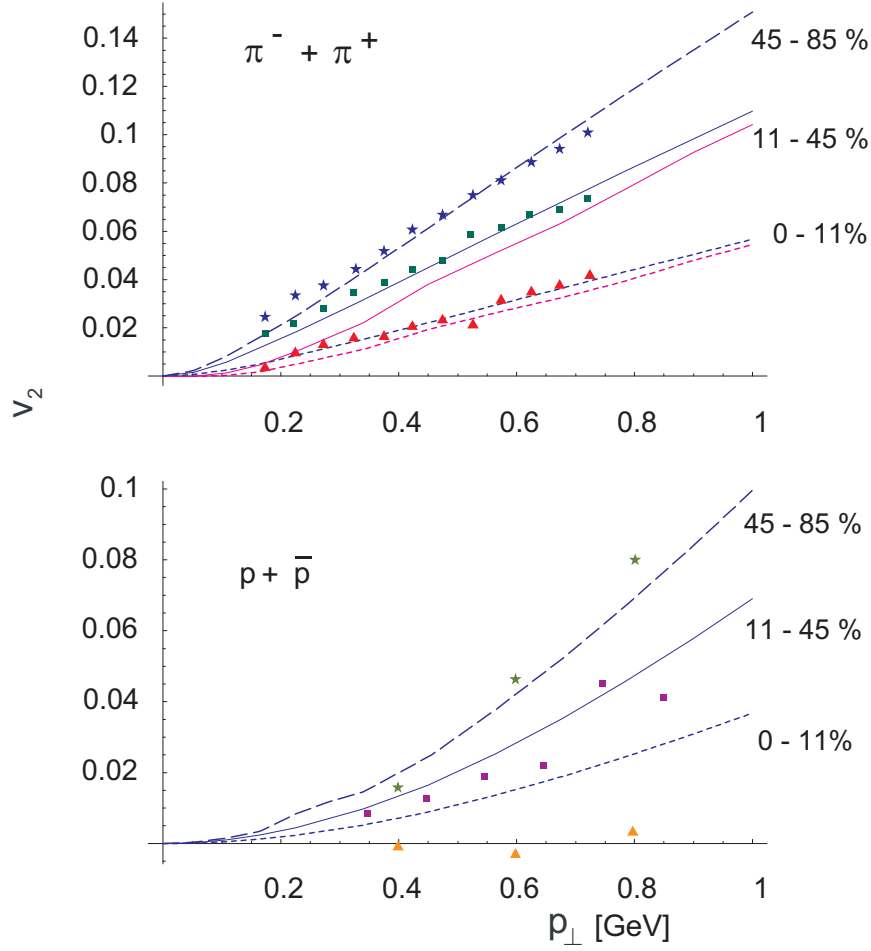


FIGURE 5. Dependence of v_2 integrated over c for identified particles on the transverse momentum, p_{\perp} . Thick (thin) lines correspond to the calculation with (without) resonance decays. Experimental points come from the STAR collaboration at $\sqrt{s_{NN}} = 130$ GeV [12]. The taken values for the shape-asymmetry parameter ε are, from the lowest to highest centrality bin, 0.08, 0.25, and 0.52, while the fitted values of the flow-asymmetry parameter δ are 0.15, 0.35, and 0.52, respectively.

where $\{\cdot\}$ denotes averaging over events, p_1 and p_2 are the momenta of the pions, $\vec{q} = \vec{p}_2 - \vec{p}_1$, and $\vec{P} = \vec{p}_1 + \vec{p}_2$. We use the Bertch-Pratt parameterization [21, 22, 23],

$$C(\vec{q}, \vec{P}) = 1 + \lambda e^{-\left(q_{\text{out}}^2 R_{\text{out}}^2 + q_{\text{side}}^2 R_{\text{side}}^2 + q_{\text{long}}^2 R_{\text{long}}^2 + 2q_{\text{out}} q_{\text{long}} R_{\text{ol}}^2\right)}. \quad (8)$$

First, let us briefly recall the experimental highlights. Two facts came as a great surprise with the RHIC data. First, the R_{side} and R_{out} radii practically do not depend on the collision energy [8, 16], and acquire similar values from AGS to RHIC, despite the increase of the energy by almost two orders of magnitude. Secondly, the ratio of R_{out} to R_{side} , which can be interpreted as a measure of the duration time of the freeze-out, is close or even less than one. This is in contradiction to anticipations from numerous hydrodynamic simulations, which had predicted $R_{\text{out}}/R_{\text{side}}$ significantly larger than one.

Our model evaluation of the correlation function is performed according to the formalism of Ref. [24], with a technical approximation of neglecting the finite life-time of resonances. In that case

$$C(\vec{q}, \vec{P}) = 1 + \frac{|\int d\Sigma(x) \cdot u(x) e^{iq \cdot x} S(P \cdot u(x))|^2}{\int d\Sigma \cdot u S((P + \frac{q}{2}) \cdot u(x)) \int d\Sigma \cdot u S((P - \frac{q}{2}) \cdot u(x))}, \quad (9)$$

where the source function is

$$S(p \cdot u) = \frac{1}{(2\pi)^3} e^{-(p \cdot u - \mu)/T} + \text{contribution from resonances}. \quad (10)$$

As discussed in Ref. [25], our model values for the geometric parameters τ and ρ_{\max} are low, of the order of the size of the colliding nuclei. As a result, the values of the R_{side} and R_{out} HBT radii obtained with the procedure described above are about 30% too low compared to the experiment. The problem can be alleviated with the inclusion of the excluded-volume (Van der Waals) corrections. Such effects have been realized to be important since the early thermal studies of the particle production in relativistic heavy-ion collisions [26, 27, 28, 29], where they led to a significant dilution of system. In the case of the Boltzmann statistics, which is a very good approximation in our case [30], the excluded volume corrections bring in a factor [28]

$$\frac{e^{-Pv_i/T}}{1 + \sum_j v_j e^{-Pv_j/T} n_j}, \quad (11)$$

into the phase-space integrals, where P is the pressure, $v_i = 4\frac{4}{3}\pi r_i^3$ is the excluded volume for the particle of species i , and n_i is the density of particles of species i . The pressure can be calculated self-consistently from the equation

$$P = \sum_i P_i^0(T, \mu_i - Pv_i/T) = \sum_i P_i^0(T, \mu_i) e^{-Pv_i/T}, \quad (12)$$

where P_i^0 denotes the partial pressure of the ideal gas of hadrons of species i . With the simplest assumption that the excluded volumes for all particles are equal, $r_i = r$, the excluded-volume correction manifests itself as a common scale factor, which we may denote by S^{-3} . The Frye-Cooper formula can then be written in the form [31, 32]

$$\begin{aligned} \frac{dN_i}{d^2p_{\perp} dy} &= \tau^3 \int_{-\infty}^{+\infty} d\alpha_{\parallel} \int_0^{\rho_{\max}/\tau} \sinh\alpha_{\perp} d(\sinh\alpha_{\perp}) \\ &\times \int_0^{2\pi} d\xi p \cdot u S^{-3} f_i(p \cdot u), \end{aligned} \quad (13)$$

where $p \cdot u = m_{\perp} \cosh\alpha_{\parallel} \cosh\alpha_{\perp} - p_{\perp} \cos\xi \sinh\alpha_{\perp}$. As can be immediately seen from this expression, the presence of the factor S^{-3} in Eq. (13) may be compensated by rescaling ρ and τ by the factor S . That way the system becomes more dilute and larger in such a way, that the *particle multiplicities and the spectra are left intact*.

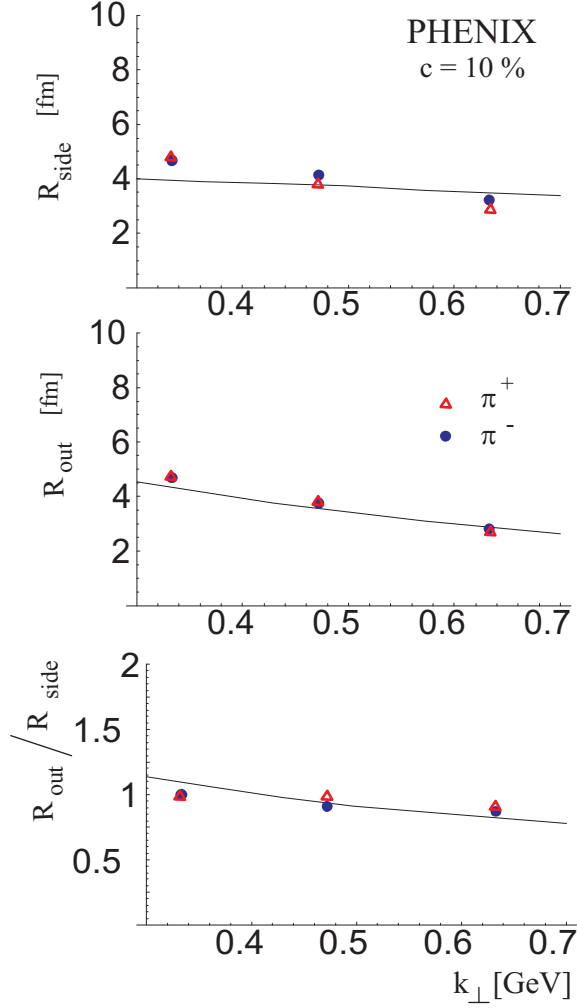


FIGURE 6. Model predictions for the pionic R_{side} and R_{out} HBT correlation radii (top two panels), and their ratio (bottom panel), confronted with the PHENIX data Au + Au data at $\sqrt{s_{NN}} = 130$ GeV and average centrality 10%. The quantity k_{\perp} is the total momentum of the pion pair.

With our values of the thermodynamic parameters $\sum_i P_i^0(T, \mu_i) = 80$ MeV/fm³, and we find $S = 1.3$ with $r = 0.6$ fm. Such a value of the excluded volume is compatible with values typically obtained in other calculations. The increase of the size parameters by 30% is what we need to bring the values of R_{side} and R_{out} up to the experimental ballpark.

Our results are shown in Fig. 6. We note that the agreement with data is very reasonable. In particular, the ratio of $R_{\text{out}}/R_{\text{side}}$ is close to one, and drops below one at larger values of the pair momentum k_{\perp} . The plots of R_{side} and R_{out} include the excluded-volume correction factor $S = 1.3$. We observe that these radii decrease with the pair momentum k_{\perp} , although somewhat slower than indicated by the data. We note that the radius R_{long} cannot be reliably evaluated in our model. This is due to the assumption of the boost invariance, *cf.* Eq. (I.2), which leads to too large values of R_{long} .

CONCLUSION

To conclude, we list the main results of our approach:

1. The thermal model works for the particle ratios, see (I).
2. Supplied with expansion, it works for the p_{\perp} -spectra, see (I). The complete treatment of resonances is essential, and the assumption of single freeze-out leads to good predictions. Moreover, the strange particles, including Ω , are described properly with no need for extra parameters.
3. Supplied with azimuthal asymmetry, the model can be used to describe the elliptic flow at moderate transverse momenta, up to $p_{\perp} \sim 2$ GeV. The fitted values of the velocity asymmetry parameter, δ , are reasonable.
4. Supplied with the excluded-volume corrections, the model works also for the HBT radii R_{side} and R_{out} . In particular, the ratio of $R_{\text{out}}/R_{\text{side}}$ is close to 1.
5. The description is efficient, involving two thermal parameters T and μ_B , two size parameters τ and ρ_{max} , and in the case of azimuthal asymmetry, two deformation parameters, ε and δ .
6. Finally, we note that the model also works for the case of RHIC at $\sqrt{s_{NN}} = 200$ GeV A as well as for SPS at $\sqrt{s_{NN}} = 17$ GeV [33, 34].

ACKNOWLEDGMENTS

This research has been supported by PRAXIS XXI/BCC/429/94, and by the Polish State Committee for Scientific Research (KBN), grants 2 P03B 11623 and 2 P03B 09419.

REFERENCES

1. Florkowski, W., and Broniowski, W. (2002), preceding talk.
2. Kolb, P. F., Sollfrank, J., Ruuskanen, P. V., and Heinz, U. W., *Nucl. Phys.*, **A661**, 349–352 (1999).
3. Voloshin, S. A., and Poskanzer, A. M., *Phys. Lett.*, **B474**, 27–32 (2000).
4. Kolb, P. F., Huovinen, P., Heinz, U. W., and Heiselberg, H., *Phys. Lett.*, **B500**, 232–240 (2001).
5. Hirano, T., *Phys. Rev. Lett.*, **86**, 2754–2757 (2001).
6. Magas, V. K., Csernai, L. P., and Strottman, D. D. (2000), nucl-th/0009049.
7. Broniowski, W., and Florkowski, W., *Phys. Rev.*, **C65**, 024905 (2002).
8. Adler, C., et al., *Phys. Rev. Lett.*, **87**, 082301 (2001).
9. Ackermann, K. H., et al., *Phys. Rev. Lett.*, **86**, 402–407 (2001).
10. Snellings, R. J. M., *Nucl. Phys.*, **A698**, 193–198 (2002).
11. Lacey, R. A., *Nucl. Phys.*, **A698**, 559–563 (2002).
12. Adler, C., et al., *Phys. Rev. Lett.*, **87**, 182301 (2001).
13. Adler, C., et al., *Phys. Rev.*, **C66**, 034904 (2002).
14. Adcox, K., et al., *Phys. Rev. Lett.*, **86**, 3500–3505 (2001).
15. Adcox, K., et al., *Phys. Rev. Lett.*, **88**, 242301 (2002).
16. Adcox, K., et al., *Phys. Rev. Lett.*, **88**, 192302 (2002).
17. Adcox, K., *Phys. Rev. Lett.*, **89**, 212301 (2002).
18. Snellings, R. (2001), hep-ph/0111437.
19. Adler, C., et al., *Nucl. Phys.*, **A698**, 64–77 (2002).
20. Baym, G., *Acta Phys. Polon.*, **B29**, 1839–1884 (1998).

21. Pratt, S., *Phys. Rev. Lett.*, **53**, 1219–1221 (1984).
22. Pratt, S., *Phys. Rev.*, **D33**, 72–79 (1986).
23. Bertsch, G., Gong, M., and Tohyama, M., *Phys. Rev.*, **C37**, 1896–1900 (1988).
24. Bolz, J., Ornik, U., Plumer, M., Schlei, B. R., and Weiner, R. M., *Phys. Rev.*, **D47**, 3860–3870 (1993).
25. Broniowski, W., and Florkowski, W., *Phys. Rev. C*, **65**, 064905 (2002).
26. Braun-Munzinger, P., Stachel, J., Wessels, J. P., and Xu, N., *Phys. Lett.*, **B344**, 43–48 (1995).
27. Braun-Munzinger, P., Stachel, J., Wessels, J. P., and Xu, N., *Phys. Lett.*, **B365**, 1–6 (1996).
28. Yen, G. D., Gorenstein, M. I., Greiner, W., and Yang, S.-N., *Phys. Rev.*, **C56**, 2210–2218 (1997).
29. Yen, G. D., and Gorenstein, M. I., *Phys. Rev.*, **C59**, 2788–2791 (1999).
30. Michalec, M., *Thermal description of particle production in ultra-relativistic heavy-ion collisions*, Ph.D. thesis, Institute of Nuclear Physics, Kraków, Poland (2001), nucl-th/0112044.
31. Broniowski, W., and Florkowski, W., *Phys. Rev. Lett.*, **87**, 272302 (2001).
32. Broniowski, W., Baran, A., and Florkowski, W., *Acta Phys. Pol. B*, **33**, 4235 (2002).
33. Broniowski, W., and Florkowski, W., “Thermal model at RHIC: particle ratios and p_{\perp} spectra,” in *Ultrarelativistic Heavy-Ion Collisions*, edited by M. Buballa, W. Nörenberg, B.-J. Schaefer, and J. Wambach, (GSI, Darmstadt), Hirschegg, Austria, 2002, p. 146.
34. Broniowski, W., and Florkowski, W., *Acta Phys. Pol. B*, **33**, 1935 (2002).